



Universiteit  
Leiden  
The Netherlands

## Modelling the interactions of advanced micro- and nanoparticles with novel entities

Zhang, F.

### Citation

Zhang, F. (2023, November 7). *Modelling the interactions of advanced micro- and nanoparticles with novel entities*. Retrieved from <https://hdl.handle.net/1887/3656647>

Version: Publisher's Version

License: [Licence agreement concerning inclusion of doctoral thesis in the Institutional Repository of the University of Leiden](#)

Downloaded from: <https://hdl.handle.net/1887/3656647>

**Note:** To cite this publication please use the final published version (if applicable).

## **Chapter 6**

# **Machine Learning-Driven QSAR Models for Predicting the Mixture Toxicity of Nanoparticles**

Fan Zhang, Zhuang Wang, Willie J.G.M. Peijnenburg and  
Martina G. Vijver

*Published in Environment International 177 (2023), 108025.*

## Abstract

Research on theoretical prediction methods for the mixture toxicity of engineered nanoparticles (ENPs) faces significant challenges. The application of *in silico* methods based on machine learning is emerging as an effective strategy to address the toxicity prediction of chemical mixtures. Herein, we combined toxicity data generated in our lab with experimental data reported in the literature to predict the combined toxicity of seven metallic ENPs for *Escherichia coli* at different mixing ratios (22 binary combinations). We thereafter applied two machine learning (ML) techniques, support vector machine (SVM) and neural network (NN), and compared the differences in the ability to predict the combined toxicity by means of the ML-based methods and two component-based mixture models: independent action and concentration addition. Among 72 developed quantitative structure-activity relationship (QSAR) models by the ML methods, two SVM-QSAR models and two NN-QSAR models showed good performance. Moreover, an NN-based QSAR model combined with two molecular descriptors, namely enthalpy of formation of a gaseous cation and metal oxide standard molar enthalpy of formation, showed the best predictive power for the internal dataset ( $R^2_{\text{test}} = 0.911$ , adjusted  $R^2_{\text{test}} = 0.733$ ,  $RMSE_{\text{test}} = 0.091$ , and  $MAE_{\text{test}} = 0.067$ ) and for the combination of internal and external datasets ( $R^2_{\text{test}} = 0.908$ , adjusted  $R^2_{\text{test}} = 0.871$ ,  $RMSE_{\text{test}} = 0.255$ , and  $MAE_{\text{test}} = 0.181$ ). In addition, the developed QSAR models performed better than the component-based models. The estimation of the applicability domain of the selected QSAR models showed that all the binary mixtures in training and test sets were in the applicability domain. This study



## 6.1 Introduction

The unique physicochemical features of nanostructured materials make them particularly appealing for specific applications (Wyrzykowska et al., 2022). Developments go with a fast pace, with first-generation nanomaterials (NMs) already embedded in a variety of products and advanced NMs such as nanocomposites continuously generated (Jayaramulu et al., 2022). With the continuous development and application of NMs, different types of engineered nanoparticles (ENPs) will now be co-discharged into the environment. Municipal wastewater treatment facilities and sewage systems are becoming crucial intermediary routes for the release of the mixtures of ENPs into the environment (Georgantzopoulou et al., 2020; Simelane and Dlamini, 2019; Singh and Kumar, 2020). It is expected that industrial and municipal wastewater are a major source of mixtures of ENPs of different compositions. As a consequence, a wide range of structurally and chemically diverse ENPs will unavoidably be released into the environmental compartments (Hong et al., 2021), raising worries about potential ENPs-induced human and ecological impacts (Avellan et al., 2021). This requires to explore the scientific challenge of assessing mixture toxicity of multiple ENPs (Zhang et al., 2022a).

Fortunately experimental data on the mixture toxicity of ENPs is expanding quite recently, while progress on methods for evaluating and predicting the mixture toxicity of ENPs is lagging (Zhang et al., 2022a). Enabling ENPs' mixture predictions, classical component-based mixture models have been used (Lopes et al., 2016; Martín-de-Lucía et al., 2019). However, these mixture models such as concentration addition (CA), independent action (IA), and a

combination of the two models rely on the assessment of the concentration-response relationship of the single components and on the identification of the toxic mode of action of the single components (F. Zhang et al., 2021b). *In silico* predictive toxicology appears to be a promising alternative to the mixture modeling. Among the novel approach methodologies based on *in silico* predictions, quantitative structure-activity relationships (QSAR) modeling proves to be a useful tool for the prediction of the biological activity or property of a compound by providing a mathematical correlation with its structural features (Tropsha, 2010). Recently, QSAR methods are being applied in methodological studies for the quantitative prediction of the toxicity of mixtures of ENPs (Kar et al., 2022; Mikolajczyk et al., 2016; Na et al., 2023; Zhang et al., 2022b). Meanwhile, machine learning (ML) methods, which seek to construct an explicit or implicit model based on current data (known as training data) to make predictions or decisions on complicated issues (M. Wang et al., 2021), have already stepped into the spotlight for *in silico* prediction of toxicology. ML methods to date have shown unprecedented predictive power in predicting the toxicity of ENPs (Balraadjsing et al., 2022; Ji et al., 2022; Jia et al., 2021; Trinh et al., 2022). Thus, ML-powered QSAR modeling approaches could be a strong tool to deal with the problem of predicting the toxicity of mixtures of ENPs, and would perform better and more cost-effective than the classical mixture models. However, there is still a scarcity of QSAR models based on ML approaches for predicting the mixture toxicity of multiple ENPs.

The present study aimed at rebuilding existing QSAR for use with NMs (nano-QSAR) by incorporating ML methods to describe the toxicity of a mixture of ENPs and comparing the performance with

the mixture models. This enables the understanding of the link between the physicochemical properties describing the components in the mixture and the cytotoxicity of 22 binary mixtures of metal oxide nanoparticles (MO<sub>x</sub> NPs) against *Escherichia coli*, a commonly used bacterium species in toxicity screening. Toxicity data for 12 binary mixtures with two different mixing ratios from our laboratory were used as an internal dataset. Toxicity data for 10 binary mixtures with another mixing ratio from the literature were used as an external dataset. The selected ML methods, namely support vector machine (SVM) (Ban et al., 2022; Liu et al., 2013) and neural network (NN) (Yang et al., 2022), are well-known and commonly utilized ML algorithms. The study involves eight indicative physicochemical parameters implicated in the mechanism of toxicity of MO<sub>x</sub> NPs: surface charge, dispersion stability, dissolution, oxidative stress, and particle reactivity. Then, for the first time, SVM- and NN-based QSAR models for predicting the cytotoxicity of mixtures of individual MO<sub>x</sub> NPs with diverse metal elements and different mixture ratios were developed. The goal of this study is to develop a rapid and cost-effective model for predicting the toxicity of mixtures of ENPs and provide a more suitable method for the risk assessment of multiple ENPs.

## **6.2 Materials and methods**

### **6.2.1 Experimental sections**

#### ***Test materials***

CuO NPs with a primary size of 40 nm (advertised specific surface area > 10 m<sup>2</sup>/g; purity 99 %), ZnO NPs with a primary size of 14 nm (advertised specific surface area of 30 ± 5 m<sup>2</sup>/g; purity > 99 %), TiO<sub>2</sub>

NPs with a primary size of  $21 \pm 5$  nm (advertised specific surface area  $50 \pm 10$  m<sup>2</sup>/g; purity > 99.5 %), and ZrO<sub>2</sub> NPs with a primary size of 5–25 nm (advertised specific surface area  $130 \pm 20$  m<sup>2</sup>/g; purity > 97.2 %) were purchased from PlasmaChem GmbH (Berlin, Germany). The MO<sub>x</sub> stock suspensions were freshly prepared in pure water after 30 min sonication in a water bath sonicator and then stored at 4 °C until use.

### ***Physicochemical analysis***

Zeta potential ( $\zeta$ P) and hydrodynamic diameters ( $D_H$ ) of the MO<sub>x</sub> NP suspensions at 10 mg/L were analyzed in water using a ZetaSizer instrument (Nano ZS90, Malvern Instruments Ltd., Worcestershire, UK).

### ***Toxicity testing***

Cytotoxicity tests were performed with *E. coli* using the microtitration plate assay (Patton et al., 2006). The initial number of bacteria was set at  $1 \times 10^8$  cells/mL. Bacterial solution after exposure to the test materials was added into a 96-well white flat-bottom microplate, which subsequently was maintained at 37 °C with shaking incubation for 12 h in a constant temperature shaker. Bacteria were exposed to increasing concentrations of the suspensions of CuO NPs (from  $1.26 \times 10^{-4}$  to  $3.02 \times 10^{-3}$  mol/L), ZnO NPs (from  $6.14 \times 10^{-5}$  to  $6.76 \times 10^{-4}$  mol/L), TiO<sub>2</sub> NPs (from  $3.76 \times 10^{-4}$  to  $3.76 \times 10^{-3}$  mol/L), and ZrO<sub>2</sub> NPs (from  $4.06 \times 10^{-4}$  to  $9.74 \times 10^{-3}$  mol/L). Each test concentration was replicated four times. The optical density (OD) values corresponding to the cell number of *E. coli* were monitored using an enzyme-labeled instrument (Thermo Multiskan FC, USA), and the



inhibition rate was calculated from the measured OD values. The cytotoxicity of the tested materials was expressed in terms of effect concentrations ( $EC_{50}$  and  $EC_{10}$ : the effective concentration of a toxicant that induces 50 and 10 % bacteria inhibition), which were calculated using a concentration-response curve (CRC). For the binary mixtures in the internal dataset, *E. coli* cells were treated with various concentrations of  $MO_x$  NPs with a fixed mixture ratio, where the first and second mixtures were based on the initial  $EC_{50}$  and the  $EC_{10}$  of each  $MO_x$  NP, respectively. Thus, the two mixtures were named Int ( $R_1$ ) mixture and Int ( $R_2$ ) mixture.

## 6.2.2 Computational methods

### ***Determination of concentration-response curve***

The Logistic regression model, as shown in Equation 6.1, was used to fit the CRCs for single and binary  $MO_x$  NPs.

$$E = \frac{100}{\left(1 + \left(\frac{C}{EC_{50}}\right)^\theta\right)} \quad (6.1)$$

where  $E$  is the effect confined to the range of 0–100 %,  $C$  is the exposure concentration of the test materials, and  $\theta$  represents the slope parameter.

### ***Joint effect modeling***

As the most representative approaches used are the IA and CA models (Bliss, 1939; Loewe and Muischneck, 1926), which were applied to predict the toxicity (denoted  $EC_{50}$  values) of the mixtures of  $MO_x$  NPs. Throughout the modeling  $EC_{50}$  values were transformed to inverted logarithm i.e.,  $\log_1/EC_{50}$ .

The general expression shown in Equation 6.2 was used for the IA model,

$$E(C_{\text{mix}}) = 1 - \prod_{i=1}^n (1 - E(C_i)) \quad (6.2)$$

where  $E(C_{\text{mix}})$  is the effect expected at the total concentration of the mixture (scaled between 0 % and 100 %) and  $E(C_i)$  is the effect that the  $i$ th mixture component would provoke if applied singly at concentration  $C_i$ .

The total concentration of a mixture causing  $x$  % effect ( $EC_{x\text{mix}}$ ) was calculated from the CRC of the individual component using the CA model, as shown in Equation 6.3,

$$EC_{x\text{mix}} = \left( \sum_{i=1}^n \frac{P_i}{EC_{xi}} \right)^{-1} \quad (6.3)$$

where  $P_i$  is the fraction of component  $i$  in the mixture and  $EC_{xi}$  is the concentration of component  $i$  that would result in  $x$  % effect if used alone.

### ***Construction of datasets***

Two datasets were constructed for the development and validation of the predictive models. The dataset was chosen not only to take into account data sample diversity (i.e., diversity of mixed components and mixed concentration ratios), but also to reduce the variability of inter-laboratory toxicity testing conditions. The first dataset (named internal dataset) consists of experimental data from our laboratory. The internal dataset consists of 12 data rows, consisting of the binary mixtures of four  $\text{MO}_x$  NPs ( $\text{CuO}$ ,  $\text{ZnO}$ ,  $\text{TiO}_2$ , and  $\text{ZrO}_2$ ) at two different mixture ratios. The results of physicochemical analysis which included the assessment of the  $\zeta\text{P}$  and the  $D_H$  of  $\text{MO}_x$  NPs in

the single and binary mixture systems and the CRCs for the mixtures obtained from the *E. coli* toxicity testing and predicted by the IA and CA models are described in the Appendix.

The second dataset (named combined dataset) comprised both internal data and external data. The external data of the toxicity of 10 binary mixtures of five MO<sub>x</sub> NPs (Al<sub>2</sub>O<sub>3</sub>, Fe<sub>2</sub>O<sub>3</sub>, SiO<sub>2</sub>, TiO<sub>2</sub>, and ZnO) to *E. coli* was collected from Kar et al. (2022). The binary nano-mixtures in the external dataset and the internal dataset have both different kinds of combinations and different mixture ratios of components between them. The external dataset was named Ext (R3) mixture. The combined dataset has a total of 22 data rows.

### ***Calculation of mixture descriptors***

A mixture descriptor ( $D_{\text{mix}}$ ) is a weighted descriptor that quantifies how much each component contributes to the overall activity of a mixture (Altenburger et al., 2003).  $D_{\text{mix}}$  has been practically applied in the toxicity prediction studies of ENP mixtures (Kar et al., 2022; Trinh et al., 2022).  $D_{\text{mix}}$  is expressed by arithmetic mean (Equation 6.4):

$$D_{\text{mix}} = x_i D_i + x_j D_j \quad (6.4)$$

where  $x_i$  and  $x_j$  are the mole fractions of constituent  $i$  and  $j$  in the mixtures, and  $D_i$  and  $D_j$  are descriptors of the individual MO<sub>x</sub> NPs. The selected descriptors of the individual MO<sub>x</sub> NPs and the calculated  $D_{\text{mix}}$  based on Equation 6.4 are shown in the Appendix Table S6.1 and Table S6.2, respectively. In the selection of descriptors for the individual MO<sub>x</sub> NPs, we referred to the qualities summarized by Roy et al. (2015). Moreover, the selected descriptors are universal

descriptors, which are effectively used to construct QSAR models of individual MO<sub>x</sub> NPs. Furthermore, these descriptors not only reflect the characteristics of nanostructures but also directly respond to toxicologically relevant properties. In details, there were eight descriptors of the individual MO<sub>x</sub> NPs from three different types: two periodic table-based descriptors (electronegativity of metal atoms,  $\chi_{me}$  and sum of metal electronegativity for an individual metal oxide divided by the number of oxygen atoms present in a particular metal oxide,  $\Sigma\chi_{me/no}$ ) derived from the publicly available periodic table information (Kar et al., 2014), two experimental descriptors ( $\zeta_P$  and  $D_H$ ) determined in our laboratory (CuO, ZnO, TiO<sub>2</sub>, and ZrO<sub>2</sub> NPs) and obtained from a previous study (Al<sub>2</sub>O<sub>3</sub>, Fe<sub>2</sub>O<sub>3</sub>, SiO<sub>2</sub>, TiO<sub>2</sub>, and ZnO NPs) (Kar et al., 2022), three metal oxide energy descriptors including the enthalpy of formation of a gaseous cation having the same oxidation state as the oxidation state of the metal in the metal oxide structure ( $\Delta H_{me+}$ ) (Puzyn et al., 2011), the metal oxide standard molar enthalpy of formation ( $\Delta H_{sf}$ ) (Haynes, 2011), and the energy of the conduction band ( $E_C$ ) (Zhang et al., 2012) of the nanoparticle, as well as the ionic index of the metal cation ( $Z^2/r$ ) (Walker et al., 2003). Stepwise multiple linear regression in SPSS 23.0 was used to perform a preliminary screening of the descriptions obtained, and the  $t$  value was selected to determine the comparative importance of the descriptors on the toxic effect concentrations ( $\log_1/EC_{50}$ ) of binary mixtures of MO<sub>x</sub> NPs.

### ***Machine Learning-based modeling***

Two popular ML algorithms, namely SVM and NN, were used to develop the QSAR models for predicting the toxicity of binary mixtures of MO<sub>x</sub> NPs. The datasets were divided into training (60 %

data) and test (40 % data) sets at random. For the SVM algorithm, the Gaussian radial basis function (RBF) was used. For the NN algorithm, the hyperbolic tan function for the hidden layer and the quasi-Newton method for weight optimization were applied. We used the data mining toolbox in Python for developing the ML-based predictive models (Demšar et al., 2013). To validate the models, the squared correlation coefficient ( $R^2$ ) and the adjusted squared correlation coefficient ( $R^2_{\text{adj}}$ ) between observed and predicted  $\log_1/EC_{50}$ , the root mean square error (RMSE), and the mean absolute error (MAE) of the training and test datasets were used. These statistical parameters are commonly used in current nano-QSAR studies and are widely accepted (Gajewicz et al., 2015; Kar et al., 2022; Trinh et al., 2022). Randomization tests proposed for testing the robustness of the selected models were performed using the metric  ${}^cR^2_p$  (Kar et al., 2014). If the  ${}^cR^2_p$  value is more than the stipulated threshold value of 0.5 then an acceptable model has been developed. The second-order bias-corrected Akaike Information Criterion ( $AICc$ ) index as an additional statistical measure was employed on the full set to evaluate the relationship between variables. The  $AICc$  value was calculated using *R* software.

### ***Applicability domain***

The OECD principles of QSAR validation recommend that: *A (Q)SAR should be associated with a defined domain of applicability* (OECD, 2014). The function of the applicability domain (AD) is to define the compounds that can be reliably predicted by the QSAR model, which can also be understood as the set of compounds to which the model applies. The AD in this work was generated by using the Student's *t*-distribution on Euclidean distances (structural domain) and

standardized residuals (response domain) of a training dataset to define the space where accurate predictions can be made with a specified level of confidence (Gajewicz, 2018).

## 6.3 Results and Discussion

### 6.3.1 Toxicity of binary ENP mixtures

CRCs established for the binary mixtures of CuO, ZnO, TiO<sub>2</sub>, and ZrO<sub>2</sub> NPs are shown in the Appendix Figure S6.1. Based on the curves, the log<sub>1</sub>/EC<sub>50</sub> values were determined and these are summarized in Table 6.1.

**Table 6.1.** Toxicity data of binary mixtures of MO<sub>x</sub> NPs for the internal dataset <sup>a</sup>

Mixture system of MO <sub>x</sub> NPs	Observed log <sub>1</sub> /EC <sub>50</sub> (mol/L)	Predicted log <sub>1</sub> /EC <sub>50</sub> (mol/L)					
		QSAR models				Mixture models	
		S12	S31	N12	N31	IA	CA
Int (R1)							
CuO + ZnO NPs	2.72	2.68	2.70	2.72	2.72	2.85	3.05
TiO <sub>2</sub> + ZrO <sub>2</sub> NPs	2.10	2.14	2.13	2.10	2.10	2.32	2.44
ZnO + TiO <sub>2</sub> NPs	2.17	2.20	2.18	2.18	2.18	2.96	3.00
ZnO + ZrO <sub>2</sub> NPs*	2.30	2.23	2.14	2.37	2.37	2.39	2.54
CuO + TiO <sub>2</sub> NPs*	2.77	2.81	2.80	2.88	2.80	2.70	2.80
CuO + ZrO <sub>2</sub> NPs	2.29	2.25	2.27	2.29	2.29	2.30	2.46
Int (R2)							
CuO + ZnO NPs*	2.82	2.68	2.70	2.69	2.66	2.92	3.15
TiO <sub>2</sub> + ZrO <sub>2</sub> NPs*	2.11	2.14	2.13	2.11	2.10	2.32	2.44
ZnO + TiO <sub>2</sub> NPs	2.20	2.21	2.18	2.19	2.18	2.77	3.05
ZnO + ZrO <sub>2</sub> NPs	2.37	2.23	2.14	2.37	2.37	2.39	2.54
CuO + TiO <sub>2</sub> NPs	2.74	2.71	2.72	2.75	2.75	2.70	2.80
CuO + ZrO <sub>2</sub> NPs	2.14	2.21	2.18	2.14	2.15	2.31	2.41

<sup>a</sup> \* indicates the test data.

For the binary mixtures with a certain mixture ratio, TiO<sub>2</sub> and ZrO<sub>2</sub> NPs induced the least toxicity in the combined exposure setting. Comparative analysis also revealed that the toxicity of CuO NPs combined with ZnO or TiO<sub>2</sub> NPs was higher than for other binary combinations.

### 6.3.2 Machine learning-based QSAR prediction

Based on the ML methods, 72 QSAR models integrating different  $D_{\text{mix}}$  (Figure 6.1) were developed. The performance of 36 SVM-and 36 NN-based QSAR models is shown in the Appendix Tables S6.3 and S6.4, respectively.

	$\chi_{me}$								
$\chi_{me}$	S1/N1	$\Sigma\chi_{me/nO}$							
$\Sigma\chi_{me/nO}$	S9/N9	S2/N2	$\zeta P$						
$\zeta P$	S10/N10	S16/N16	S3/N3	$D_H$					
$D_H$	S11/N11	S17/N17	S22/N22	S4/N4	$\Delta H_{me+}$				
$\Delta H_{me+}$	S12/N12	S18/N18	S23/N23	S27/N27	S5/N5	$\Delta H_{sf}$			
$\Delta H_{sf}$	S13/N13	S19/N19	S24/N24	S28/N28	S31/N31	S6/N6	$E_C$		
$E_C$	S14/N14	S20/N20	S25/N25	S29/N29	S32/N32	S34/N34	S7/N7	$Z^2/r$	
$Z^2/r$	S15/N15	S21/N21	S26/N26	S30/N30	S33/N33	S35/N35	S36/N36	S8/N8	

**Figure 6.1.** SVM (S1–S36)- and NN (N1–N36)-based QSAR models prepared from the pool of different mixture descriptors.  $\chi_{me}$  – metal electronegativity,  $\Sigma\chi_{me/nO}$  – sum of metal electronegativity for individual metal oxide divided by the number of oxygen atoms present in particular metal oxide,  $\zeta P$  – zeta potential,  $D_H$  – hydrodynamic diameters,  $\Delta H_{me+}$  – enthalpy of formation of a gaseous cation,  $\Delta H_{sf}$  – metal oxide standard molar enthalpy of formation,  $E_C$  – nanoparticle energy of conduction band, and  $Z^2/r$  – ionic index of metal cation.

We selected a good prediction model according to the following three criteria: (i)  $R^2 \geq 0.81$  for *in vitro* data (Kubinyi, 1993); (ii) adjusted  $R^2 > 0.60$  (Olasupo et al., 2020); (iii) the above two conditions need

to be satisfied not only for both the training and the test sets but also for both the internal and combined datasets, as well as for both the SVM- and NN-based models when applying the same descriptors. Among the developed QSAR models, two SVM-based models (S12 and S31) and two NN-based models (N12 and N31) performed comparably better than other models for both the internal and combined datasets. This also means that the selected QSAR models can reliably predict the toxicity of mixtures of individual MO<sub>x</sub> NPs under multiple different experimental conditions.

Moreover, the predicted  $\log_1/EC_{50}$  values by the good models (S12, S31, N12, and N31) are shown in Table 6.1 (the internal dataset) and in Table 6.2 (the combined dataset). The percental difference averaged between the experimental and predicted values by the selected models for the internal and combined datasets was 2.34, 2.50, 1.08, 1.04 and 7.16, 7.29, 2.87, 2.61 % respectively. In addition, the obtained  ${}^cR^2_P$  values for the selected models via the Y-randomization test are higher than 0.5 (Appendix Tables S6.5 and S6.6), demonstrating that the models were not created randomly and that they are robust.

Experimentally determined  $\log_1/EC_{50}$  are plotted against predicted  $\log_1/EC_{50}$  for the internal and combined datasets (Figure 6.2 and Figure 6.3, respectively). The green dotted line indicates that the experimental and the predicted values correspond exactly. The blue straight line depicts a linear relationship between the experimental and predicted values based on the training sets.



**Table 6.2.** Toxicity data of binary mixtures of MOx NPs for the combined dataset <sup>a</sup>

Mixture system of MO <sub>x</sub> NPs	Observed log <sub>1</sub> /EC <sub>50</sub> (mol/L)	Predicted log <sub>1</sub> /EC <sub>50</sub> (mol/L)			
		QSAR models			
		S12	S31	N12	N31
Int (R1)					
CuO + ZnO NPs	2.72	2.80	2.89	2.72	2.72
TiO <sub>2</sub> + ZrO <sub>2</sub> NPs	2.10	2.18	2.05	2.10	2.11
ZnO + TiO <sub>2</sub> NPs*	2.17	1.92	2.09	2.21	2.18
ZnO + ZrO <sub>2</sub> NPs	2.30	2.22	2.13	2.30	2.30
CuO + TiO <sub>2</sub> NPs	2.77	2.82	2.94	2.77	2.77
CuO + ZrO <sub>2</sub> NPs	2.29	2.27	2.47	2.27	2.26
Int (R2)					
CuO + ZnO NPs*	2.82	2.88	2.92	2.74	2.75
TiO <sub>2</sub> + ZrO <sub>2</sub> NPs*	2.11	2.18	2.05	2.11	2.11
ZnO + TiO <sub>2</sub> NPs	2.20	1.92	2.10	2.19	2.18
ZnO + ZrO <sub>2</sub> NPs*	2.37	2.22	2.13	2.30	2.30
CuO + TiO <sub>2</sub> NPs*	2.74	2.27	2.58	2.05	2.50
CuO + ZrO <sub>2</sub> NPs	2.14	2.22	2.31	2.17	2.19
Ext (R3)					
Al <sub>2</sub> O <sub>3</sub> + ZnO NPs	4.26	3.93	3.88	4.26	4.26
Al <sub>2</sub> O <sub>3</sub> + Fe <sub>2</sub> O <sub>3</sub> NPs	2.06	2.14	2.01	2.06	2.07
Al <sub>2</sub> O <sub>3</sub> + SiO <sub>2</sub> NPs*	1.71	1.86	1.85	1.88	1.54
Al <sub>2</sub> O <sub>3</sub> + TiO <sub>2</sub> NPs	1.70	1.95	1.87	1.71	1.70
ZnO + Fe <sub>2</sub> O <sub>3</sub> NPs	3.89	3.81	3.72	3.89	3.89
ZnO + SiO <sub>2</sub> NPs	4.13	3.62	3.57	4.13	4.13
Fe <sub>2</sub> O <sub>3</sub> + SiO <sub>2</sub> NPs	2.25	2.17	2.08	2.25	2.25
Fe <sub>2</sub> O <sub>3</sub> + TiO <sub>2</sub> NPs*	1.99	1.75	2.10	1.72	2.28
SiO <sub>2</sub> + TiO <sub>2</sub> NPs	1.80	1.88	2.01	1.81	1.80
ZnO + TiO <sub>2</sub> NPs*	4.59	3.76	3.69	4.46	4.01

<sup>a</sup> \* indicates the test data.

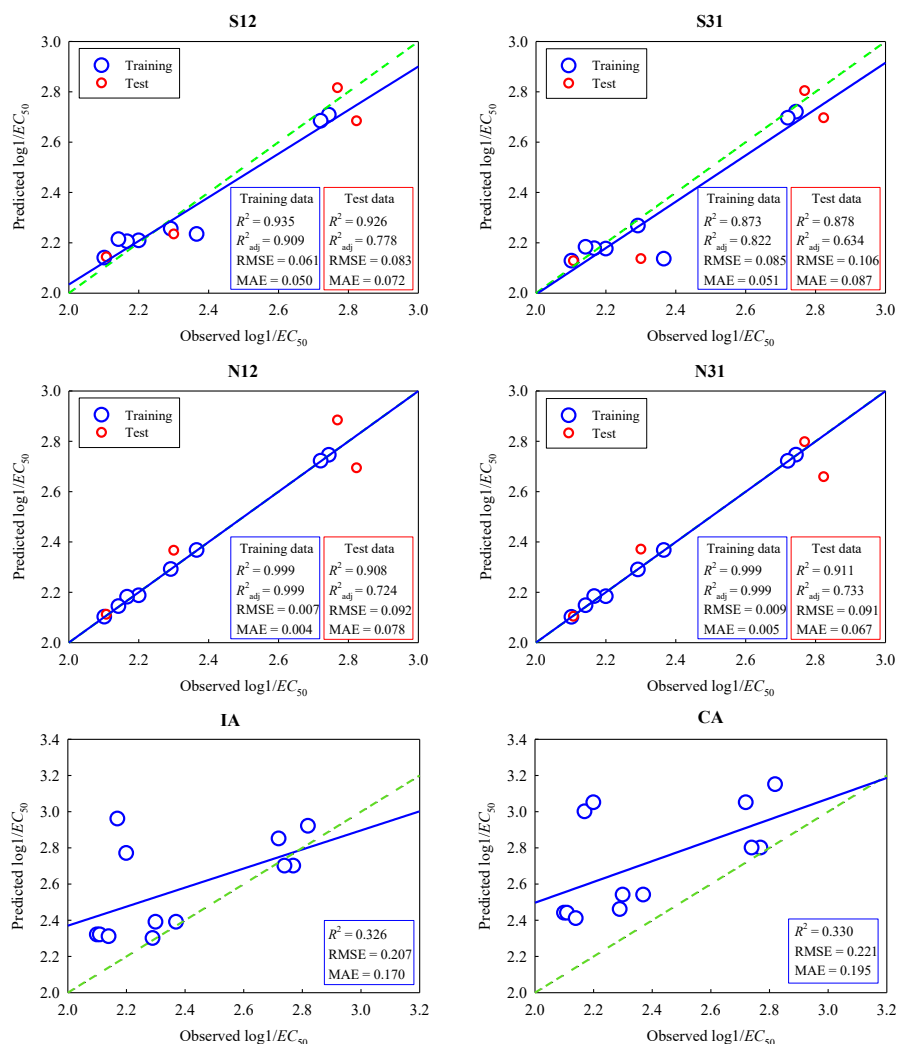


**Figure 6.2.** Performance of the selected SVM- and NN-based QSAR models and the component-based mixture models developed based on the internal dataset.

In general, the selected QSAR models exhibited good agreement ( $R^2 \geq 0.81$ ) between the observed and predicted toxicity for the binary mixtures of MO<sub>x</sub> NPs from the training set (blue circle) and those from the test sets (red circle). It can also be seen that the lines of the regression for the N12 and N31 models overlap with the line of

perfection, implying that the NN-based models showed better consistency between the experimental and predicted values compared to the SVM-based models. Furthermore, the percental difference averaged between the experimental and predicted values by the NN-based models was 2.17–2.40 and 2.49–2.79 times lower than the percental difference averaged between the experimental and predicted values by the SVM-based models in the internal (Appendix Table S6.7) and combined datasets (Appendix Table S6.8), respectively. Note that the N31 model had the lowest average difference between the experimental and predicted values among the selected QSARs.

In addition, the results for the statistics of the selected models are shown in the insets of Figures 6.2 and 6.3. In the internal dataset (Figure 6.2), the S12 model with higher  $R^2_{\text{adj}}$  and lower RMSE and MAE performed better than the S31 and N12 models for predicting the test data. In addition to this, the NN-based models showed better than the SVM-based models for predicting both the training and test data. Further comparisons revealed that the N31 model with higher  $R^2_{\text{adj}}$  and lower RMSE and MAE performed better than the N12 model for predicting the test data. In the combined dataset (Figure 6.3), the NN-based models with higher  $R^2_{\text{adj}}$  and lower RMSE and MAE outperformed the SVM-based models for both the training and test data. Of the four models validated, the N31 model with the highest  $R^2_{\text{adj}}$  and the lowest RMSE and MAE had the best performance capability for predicting the test data.

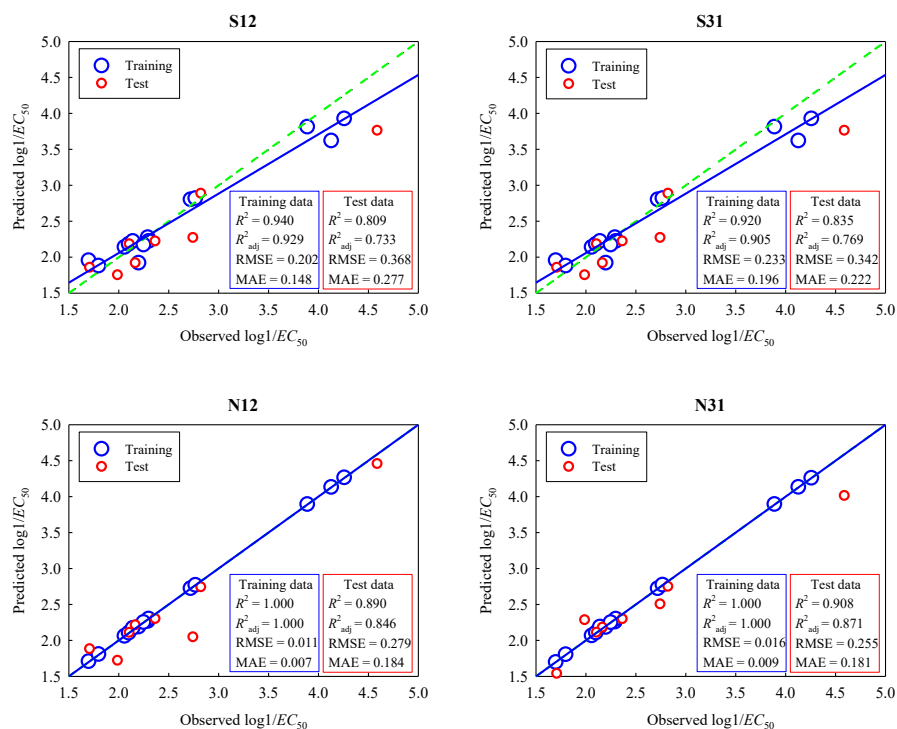


**Figure 6.3.** Performance of the selected SVM- and NN-based QSAR models developed based on the combined dataset.

Current research on biological effect prediction also indicates that NN-based models outperform SVM-based models empirically resulting from the training process and overall data prediction (Almansour et al., 2019; Bennett-Lenane et al., 2022), while other studies have shown that the SVM-based modeling approach often shows a better performance than the NN-based approach (X. Li et al., 2021; Zhao et al., 2006). In theory, both ML algorithms have advantages and disadvantages. This is reflected in that the training time for NN-based technique is higher than the training time for SVM, while the prediction time for NN models is generally lower than for SVM models. Taken together, the performance indicators of the

selected QSARs indicate that both the NN and the SVM were practical tools for the prediction of the toxicity of mixtures of ENPs.

To compare the differences between the developed QSAR models and the classical mixture models in predicting the toxicity of mixtures of MO<sub>x</sub> NPs, we also constructed the IA and CA prediction models (Appendix Figure S6.1). As shown in Figure 6.2, the selected QSAR models gave better predictions of  $\log_1/EC_{50}$  ( $R^2 \geq 0.873$ ) compared to those models based on mixture modeling making use of IA ( $R^2 = 0.326$ ) and CA ( $R^2 = 0.330$ ). This implies that the QSAR models are low-cost approach to risk assessment of multiple ENP mixtures, due to the fact that the QSAR models do not need concentration-response information on each mixture component as with the commonly applied mixture models either using IA or CA. For the CuO + ZrO<sub>2</sub> NPs mixture at ratio 1 and the ZnO + ZrO<sub>2</sub> NPs mixture at ratio 2, the percental difference averaged between the experimental and predicted values by the IA model was lower than the percental difference averaged between the experimental and predicted values by the SVM-based models (Appendix Table S6.7). This means that for a particular mixture the mixture model has the ability to predict the toxicity of the mixture of MO<sub>x</sub> NPs.

The mixture model has become a prevailing approach for the quantitative prediction of mixture toxicity with concentration addition being a conservative measure of addition of stress and independent action as assuming induced effects not at the same target and affecting a percentage at the overall response, which strengthens the theorization from the basic principles of mixture toxicology. However, the interactions between the joint chemicals are not taken into consideration in the mixture models. Especially, the

distinctive physicochemical features of ENPs, which have a high surface area for adsorption, may hinder the mixture models from accurately estimating the toxicological effects of mixtures containing ENPs (Martinez et al., 2022). A previous study indicated that the IA and CA models did not perform well in predicting the toxicity of mixtures comprising TiO<sub>2</sub> NPs and other pollutants to *Daphnia magna* (Trinh et al., 2022). Thus, it is reasonable to assume that the ML-integrated QSAR approach can be considered a highly promising tool for the assessment of the toxicity of a mixture of multiple ENPs.

### **6.3.3 Applicability domains of QSAR models**

The AD of a QSAR is the physicochemical, structural, or biological space, knowledge or information on which the training set of the model has been developed, and for which it is applicable to make predictions for new compounds (Jaworska et al., 2005). The AD of the SVM-based models (S12 and S31) and NN-based models (N12 and N31) constructed from the internal and combined datasets is shown in Figures 6.4 and 6.5, respectively. The light and dark green elliptical boundaries correspond to the 95 and 99 % confidence intervals, respectively. Reliable predictions can only be generated within these confidence intervals. In the internal dataset (Figure 6.4), all the training data fall inside the 95 % confidence area, while two test data for the S12 model and only one test data for the S31 and N31 models falls between 95 % and 99 % confidence area. In the combined dataset (Figure 6.5), all the training and testing data fall inside the 95 % confidence area. Generally, all the studied binary mixtures of MO<sub>x</sub> NPs were located within the 99 % confidence area of the selected QSAR models. Thus, the mixture toxicity predictions for each training and test mixtures of MO<sub>x</sub> NPs are highly reliable for the selected

QSAR models. This suggests that the QSAR models can be used to predict the toxicity of any other binary combinations of MO<sub>x</sub> NPs, especially because the predominant first-generation ENPs are within this training set as well as the mechanistically relevant descriptors.

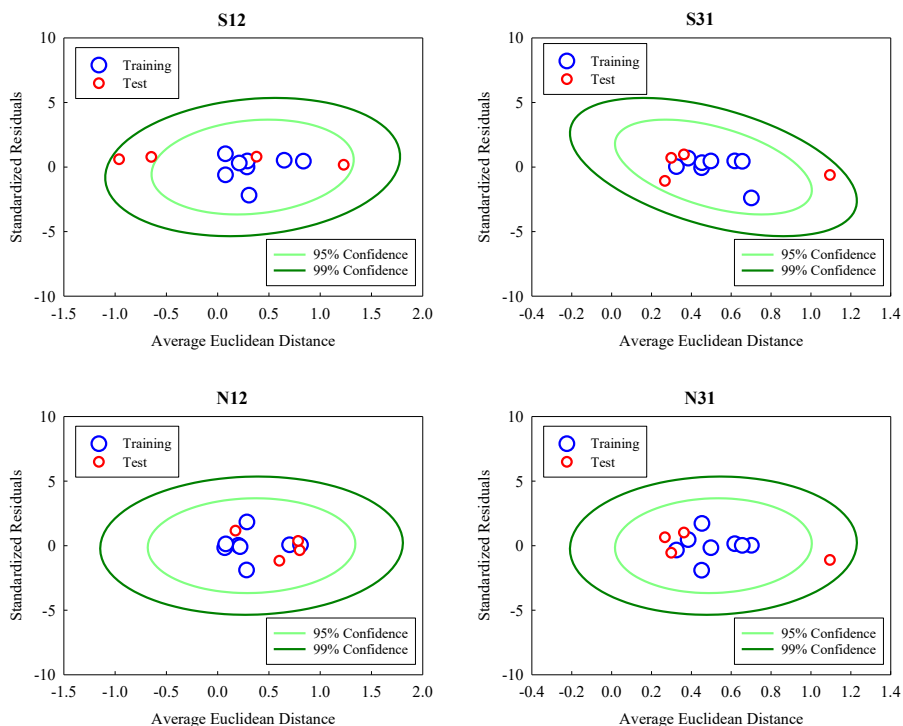


**Figure 6.4.** Applicability domains of the selected SVM- and NN-based QSAR models developed based on the internal dataset.

A QSAR model should have a well-defined AD to reflect its reliability in order to be applicable for chemical assessment and management. The dataset with 22 binary combinations has proven to be large and robust to effectively build ML-driven QSAR models for toxicity prediction. This is in line with previous conclusions confirming that ML-assisted QSAR models has good predictive power for relatively small datasets (Gajewicz et al., 2015; Puzyn et al., 2011; Zhong et al.,

2022b). These findings do give prospects of application to move the field on mixture toxicity predictions further especially when ENPs mixtures are considered in which chemicals as well as particles influence fate and responses.

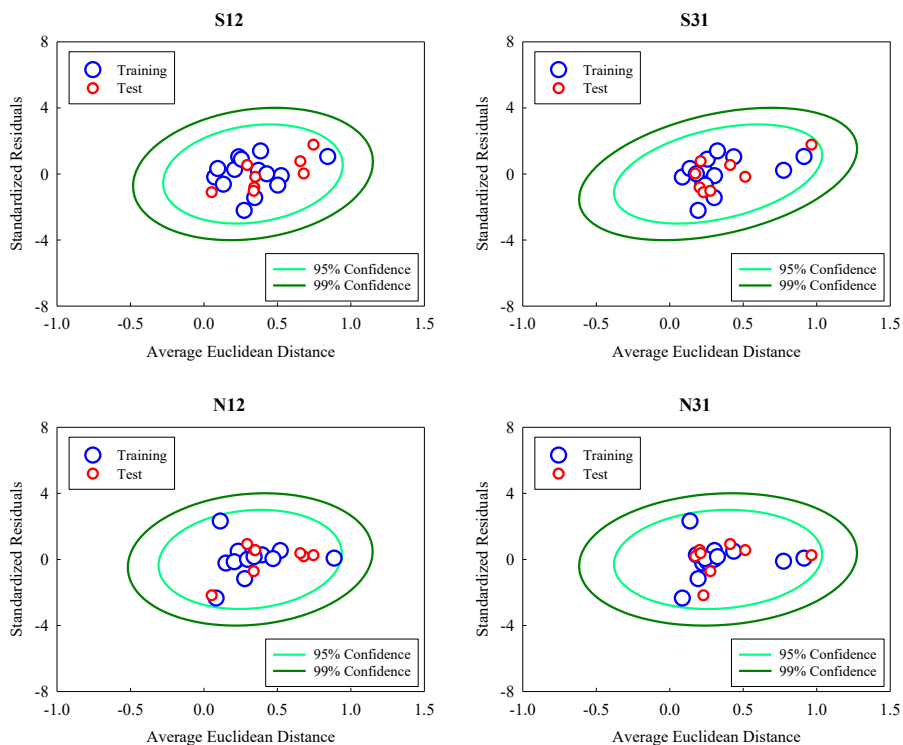


**Figure 6.5.** Applicability domains of the selected SVM- and NN-based QSAR models developed based on the combined dataset.

The characterization of the AD reflects the dependence of a QSAR model on training data (Zhong et al., 2022a). Thus, only nanostructured materials that are similar to the ENPs constituting the training set, can be reliably predicted. While artificial intelligence, ML, and big data analytics provide powerful algorithms and tools for QSAR modeling, high-quality toxicity data remain the driving force



for constructing QSAR models for the prediction of the toxicity of nano-mixtures. Therefore, further research needs to expand the amount of high-quality data available on the toxicity of mixtures of ENPs in the training set and enlarge the AD of QSAR models.

### **6.3.4 Importance of descriptors and mechanistic knowledge**

Appendix Table S6.9 shows the comparative importance of the proposed descriptors for the toxicity prediction of binary mixtures of MO<sub>x</sub> NPs. The magnitude of the relative importance of  $\Delta H_{sf}$  (62 %) and  $\Delta H_{me+}$  (47 %) is the highest in the internal and combined datasets studied respectively, suggesting that the two descriptors are very important in explaining the QSAR models. As an efficient descriptor,  $\Delta H_{me+}$  was previously employed to explain the cytotoxicity of MO<sub>x</sub> NPs to *E. coli* based on their chemical stability. The chemical stability of MO<sub>x</sub> NPs is associated with the release of metal cation from the particles as well as the catalytic properties and redox modifications of the surface (Puzyn et al., 2011). For a given size,  $\Delta H_{sf}$  might be also used as an indicator of "the ability of releasing metal cation", since it is proportional to the energy of a single metal-oxygen bond in the oxides (Gajewicz et al., 2015). The cellular damage caused by MO<sub>x</sub> NPs may be attributed to the release of metal cations. The metal ions present in suspension can not only chelate with specific ligands of biological macromolecules to affect the toxicity of MO<sub>x</sub> NPs to biological cells, but also can instigate the generation of free radicals such as hydroxyl radicals in both cells and mitochondria, causing DNA and mitochondrial DNA breakage (Roy et al., 2019).

In addition,  $\chi_{me}$  was a significant descriptor in developing the S12 and N12 models, and indicates the energy needed to separate the metal

cation from the metal oxides as part of the mechanisms underlying the toxic effects of the metal oxides.  $\text{MO}_x$  NPs with a higher  $\chi_{\text{me}}$  tend to gain electrons from the bonding pair of the electrons. This indicates an increase in the catalytic capabilities of cationic metal (Roy et al., 2019). Thus, the toxicity of  $\text{MO}_x$  NPs may be enhanced in accordance with the Haber-Weiss-Fenton cycle (Koppenol, 2001).  $\chi_{\text{me}}$  is also independent of the size range of  $\text{MO}_x$  NPs (Kar et al., 2014). Following the release of metal cations, redox interactions with the molecules in biological media frequently result in the production of reactive oxygen species (ROS) (Puzyn et al., 2011). Thus, the released cations themselves, ROS-induced oxidative damage, or both may be responsible for the observed cytotoxicity. Our results indicated that these descriptors could indicate possible mechanism for the mixture toxicity of individual  $\text{MO}_x$  NPs. What is more, the descriptors used in the models are well-defined and can be derived quickly from the chemical composition information ( $\chi_{\text{me}}$ ) and chemical stability ( $\Delta H_{\text{me}+}$  and  $\Delta H_{\text{sf}}$ ).

The *AICc* values were further applied to evaluate the relationship among the proposed descriptors ( $\chi_{\text{me}}$ ,  $\Delta H_{\text{me}+}$ , and  $\Delta H_{\text{sf}}$ ). As shown in the Appendix Table S6.10, in both the internal dataset and the combined dataset, the *AICc* value of the model developed by applying  $\Delta H_{\text{me}+}$  and  $\Delta H_{\text{sf}}$  was the smallest among all the models combined with the binary descriptors. This indicates that the fitting ability of the model incorporating  $\Delta H_{\text{me}+}$  and  $\Delta H_{\text{sf}}$  was higher than the fitting ability of the other models using the combination of two descriptors. This is generally consistent with the results of the screening and comparative analysis regarding the performance of ML models as described previously. The models developed by applying  $\Delta H_{\text{sf}}$  and

$\Delta H_{me+}$  to the internal and combined datasets, respectively, had the lowest *AICc* (Appendix Table S6.10). However, the predictive power of the ML models developed by both single descriptors cannot ensure equal predictive power for the internal dataset and the combined dataset (Appendix Tables S6.3 and S6.4).

Furthermore, we found that the *AICc* values of models developed by the combination of three descriptors ( $\chi_{me}$ ,  $\Delta H_{me+}$ , and  $\Delta H_{sf}$ ) were the highest in the internal dataset, while the *AICc* values of the models developed by the combination of three descriptors in the combined dataset were higher than those of the models developed by the single descriptor ( $\Delta H_{me+}$ ) and the combination of  $\Delta H_{me+}$  and  $\Delta H_{sf}$  (Appendix Table S6.10). This implies that applying more descriptors ( $n = 3$ ) to the model in this study could not significantly improve the predictive performance of the model. Furthermore, using fewer descriptors in QSAR analysis not only allows for avoiding over-fitting, but also establishes meaningful models with understandable chemical mechanisms (Wang and Chen, 2020). Thereupon, the suggested QSAR models with few utilized nano-descriptors can be regarded as robust and simple to use for predicting the mixture toxicity of ENPs.

## 6.4 Conclusions

Our results show that the ML methods present unprecedented opportunities and challenges for the assessment of the mixture toxicity of ENPs. The nano-QSAR models that we developed and validated, outperformed conventional mixture models. The  $\chi_{me}$ ,  $\Delta H_{me+}$ , and  $\Delta H_{sf}$  were found to be the key nano-descriptors capable of predicting the mixture toxicity. At the present stage, the synthesis of new NMs and the advanced complexity of materials has a more rapid

pace than the science to predict the fate and effects of those complexes and mixtures of ENPs. Knowledge on the mixture impacts of various shaped and chemically diverse ENPs as well as the evaluation of the environmental hazards of combinations of ENPs is a necessity to work on.

### **Acknowledgements**

The research described in this work was supported by the National Natural Science Foundation of China (grant number 31971522) and by the European Union's Horizon 2020 research and innovation program via the projects "NanoinformaTIX" (grant number 814426). Martina G. Vijver acknowledges the support of the ERC-C grant entitled EcoWizard no. 101002123. Fan Zhang greatly acknowledges the support from the China Scholarship Council (grant number 202008320308).